Integral Air Quality Assessment to resolve the PM Background: The Role of Traffic and Ammonia Emissions in Secondary Aerosol Formation

B. C. Lackner[1], U. Uhrner[1], R. Reifeltshammer[1], R. Forkel[2], P. J. Sturm[1]

[1] Institute of Internal Combustion Engines and Thermodynamics (IVT), Graz University of Technology, A-8010 Graz, Austria,
uhrner@ivt.tugraz.at
[2] Karlsruhe Institute of Technology (KIT), Institute of Meteorology and Climate Research – Atmospheric Environmental Research, D-82467 Garmisch-Partenkirchen, Germany

1. Introduction and Background

Local particulate matter (PM) concentrations can be assigned to various sources, which are commonly divided into origins for primary and secondary aerosols. Sources for primary aerosols mostly comprise local anthropogenic emissions, arising from traffic, domestic heating and from industry. They are rather tied to cities and traffic routes. Sources for secondary aerosols are various gaseous precursor substances, mostly ammonia (NH_3), sulphur dioxide (SO_2) and nitrogen oxides (NO_x) for secondary inorganic aerosols (SIA); NMVOC and biogenic precursor emissions are precursors for secondary organic aerosols (SOA). SIA account for a good share in total PM concentrations. (Spangl et al., 2006), estimated an average PM10 share of up to 50% for SIA in Austria in winter. The main fraction of secondary aerosols consists of inorganic compounds (sulphate, SO_4^{2-}, nitrate, NO_3^- and ammonium, NH_4^+).

Here, the focus is placed on ground level concentrations of primary PM and secondary inorganic aerosols (SIA) formed by chemical reactions including emissions from traffic and agriculture in southern Austria, i.e., southern Styria and large parts of Carinthia, and northern Slovenia. This region is hereinafter referred to as PMinter region (see Figure 1). The overall aim is to obtain an estimate for the PM concentration reduction potential due to decreasing emission from traffic and agriculture. The presented work was embedded in the EU-funded project PMinter[1], which aimed at supporting a sustainable improvement of air quality in this region to reduce health risks for the residents (Uhrner et al., 2014).

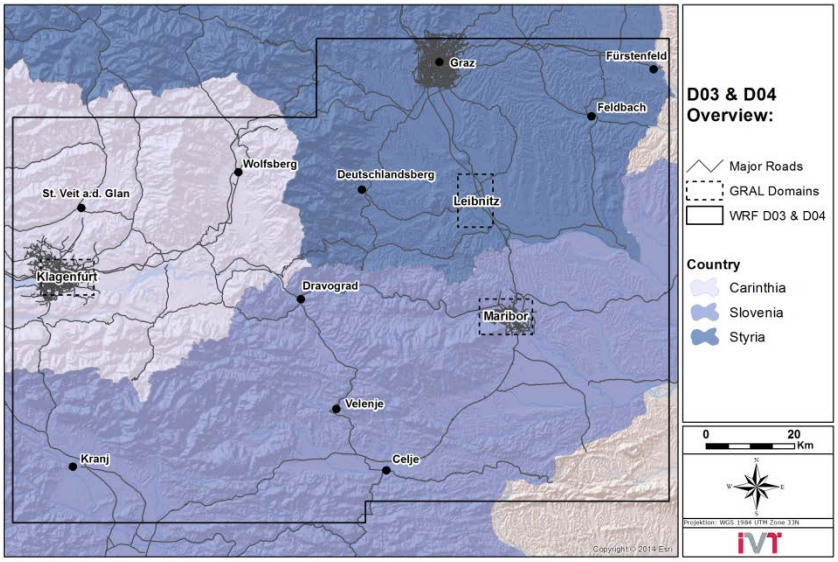

Figure 1: The PMinter project area. The solid line marks the WRF-Chem simulation region, the dotted rectangles the micro-scale focus areas

The PMinter region is crossed by some major motorways and contains cities such as Graz (approx. 250,000 inhabitants), Maribor (approx. 95,000 inhabitants), Klagenfurt (approx. 90,000 inhabitants) and Leibnitz (approx. 8000 inhabitants). The cities (with the major aerosol sources domestic heating, traffic and industry) and motorways attribute to primary aerosols, including precursor gases for the formation of SIAs. The rural areas are strongly influenced by agriculture. In the eastern part of the region, livestock breeding prevails and the emphasis is on piggery. There, high ammonia emissions facilitate the forming of SIAs.

[1] http://pminter.eu/en.html (2014-07-29)

The topography of the PMinter region can be characterized as complex terrain. Located south of the Alps, the region is shielded from weather systems steered towards Austria by northerly and westerly winds, which thus leads to rather low wind speeds and to reduced dilution of air pollutants in valleys and basins. In the cold season, air pollutants can accumulate due to frequently occurring temperature inversions. These adverse topographical and meteorological conditions lead to numerous PM10 exceedance days with respect to the EU 24-hour limit value (ECE, 2008) and the Austrian threshold (IG-L, 2011), as shown in Figure 2 (the data presented were made available by the PMinter project partners or are based on Anderl et al., 2014; Spangl and Nagl, 2012; Spangl and Nagl, 2011; Spangl and Nagl, 2010; Spangl and Nagl, 2009).

The goal of the PMinter air quality modelling efforts was to gain a better understanding of PM10 by resolving the PM concentrations levels spatially, temporally and compositionally, particularly for the cold season. In addition to the here presented issues of traffic and ammonia induced SIAs, which are discussed on a regional level, a new multi-scale model approach was developed within the project. The model was validated using concentration levels recorded at the air quality monitoring stations and the results of filter analyses from air quality measurements in three micro-scale focus areas, namely Klagenfurt, Leibnitz and Maribor (those micro-scale areas are marked by rectangles in all following figures, which show spatial data). This multi-scale model approach is based on a sophisticated combination of simulation results from a regional meteorological chemistry transport model with results from a Lagrangian dispersion model featuring a much higher spatial resolution for air pollutant concentrations. It allows for a much better local-scale estimation of total PM10 concentrations as well as a breakdown of local and regional (i.e., transported) contributions to PM10 sources, which includes the determination of local PM10 background concentrations. Further details on this model-approach can be found in Uhrner et al. (2014).

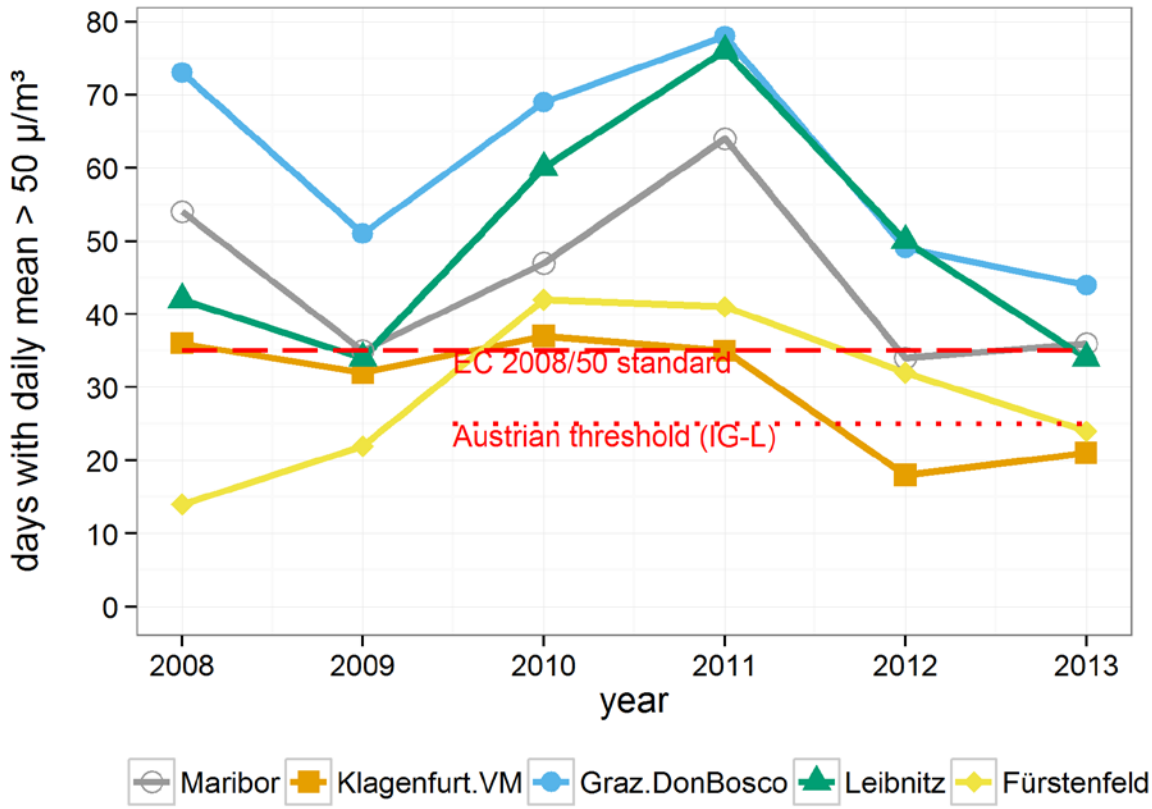

Figure 2: Yearly number of days exceeding the 50 µg m^{-3} threshold at five air quality monitoring stations. The stations Maribor, Klagenfurt.VM and Graz DonBosco are mainly influenced by city traffic, the area nearby the station Fürstenfeld is characterized by agriculture

2. Data, model and spatial-temporal setup to simulate PM and SIA

Three ingredients are needed to simulate the spatial distribution of PM and SIA concentrations: (1) a model, which describes the dispersion of air pollutants and is able to depict chemical processes in the atmosphere leading to the formation of secondary aerosols; (2) the meteorological situation in the study area, which is the driving force for dispersion processes; (3) a detailed emission data base. An overview on the ingredients is given in the following, as well as an introduction to the emission scenarios used to study the influence of emission reduction from traffic and agriculture on air pollutant concentration levels.

The regional meteorological chemistry transport model WRF-Chem

To simulate regional PM and precursor concentration levels, the Weather Research and Forecast (WRF[2]) model coupled with Chemistry (WRF-Chem; Grell et al., 2005) was employed. WRF-Chem uses a nested approach to downscale data from a European level (domain D01, horizontal resolution of about 25 km), over a trans-national level (D02, including mostly large parts of Austria and Slovenia, horizontal resolution of 5 km), to the PMinter focus region (D03a, D03b), where the horizontal resolution of the input and output data is on 1 km x 1 km (see Figure 3 for the domain nesting). This incorporation of various model scales permits not only to include local and regional emission patterns and ensuing atmospheric chemistry and aerosol dynamic processes resulting in secondary aerosols, but also comprises long-range as well as regional transport of air pollutants through system boundaries. For the PMinter project, the version 3.2.1 of WRF-Chem was used.

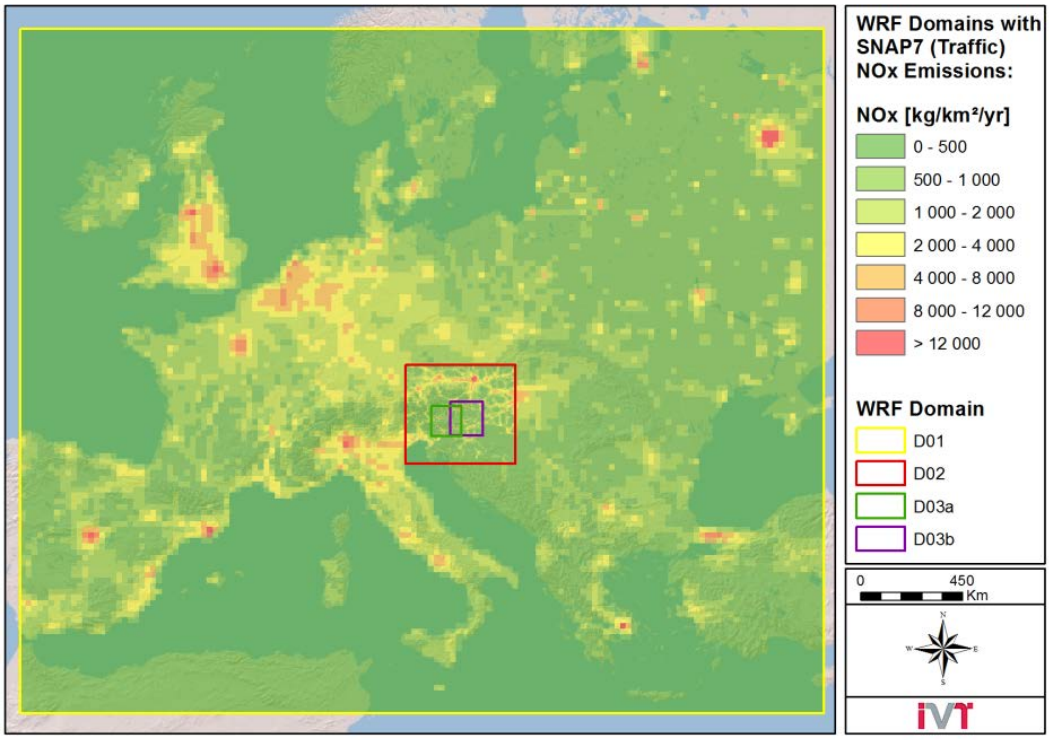

Figure 3: Boundaries of WRF-Chem domains, depicting exemplarily NOx emissions from traffic. The focus of this paper on the domains D03a and D03b, marked by green and purple rectangles.

WRF-Chem offers a wide choice of different physics and chemistry options. The physics options chosen for the meteorological part were the YSU (Yonsei University) planetary boundary layer scheme (Hong et al., 2006), the NOAH land surface model (Chen and Dudhia, 2001) to de-scribe the heat and water balance in the soil, the Rapid Radiation Transfer Mode RRTM long wave and Goddard shortwave radiation schemes (Mlawer et al., 1997; Chou and Suarez, 1994), the 3D ensemble cumulus parameterization with radiative feedback and shallow convection (Grell and Dévényi, 2002) and the cloud microphysics according to (Lin et al., 1983). For air chemistry, the RADM2 gas phase mechanism (Stockwell et al., 1990) was used. For the description of aerosol chemistry and physics, the Modal Aerosol Dynamics Model for Europe/Secondary Organic Aerosol Model (MADE/SORGAM) modules were applied (Schell et al., 2001). The RADM2–MADE/SORGAM system was chosen as it contains also organic aerosol compounds and is a good compromise between numerical costs and complexity of the physical and chemical processes that are described.

[2] www.wrf-model.org (2014-07-29)

ERA-Interim as meteorological data set

To describe the meteorological conditions during the focus period, i.e., January 2010, the ERA-Interim re-analysis data (Dee et al., 2011) from the European Centre for Medium-Range Weather Forecasting (ECMWF) were used. The last week of December 2009 was used for the model spin-up. In WRF, meteorological data provide initial and boundary conditions to simulate the transport and dispersion conditions for the European scale. ERA-Interim is one the best available meteorological databases; however, due to the still relatively coarse resolution, it shows shortcomings with respect to surface wind speeds, which are generally too high for most of the PMinter region. Figure 4 depicts exemplarily for the location of an air quality monitoring station in the city centre of Klagenfurt the WRF simulated and the observed distribution of wind directions and speeds. While the general distribution of wind directions agrees quite well with the observations at this location, the simulated wind speeds are much too strong compared to the observed ones. This may cause an overestimate of turbulent diffusion so that the dilution of air pollutants is too strong. As consequence, the simulations may underestimate the concentration levels of air pollutants. This has to be kept in mind when interpreting model results.

In addition to the overestimated wind speed, the used resolution of 1 km x 1 km in the PMinter domain (not only for meteorology, but also for the orography) is not able to resolve reasonably well small-scale topographical effects. Nevertheless, WRF-Chem is an adequate model to study the regional influence of emission changes on air pollutant concentration levels, since it includes secondary aerosol formation processes and transport through system boundaries. For local-scale analysis, the combination of WRF with a dispersion model for micro-scale issues, e.g., GRAL (Oettl and Uhrner, 2012; Oettl et al., 2003) can overcome the scale-induced shortcomings of WRF.

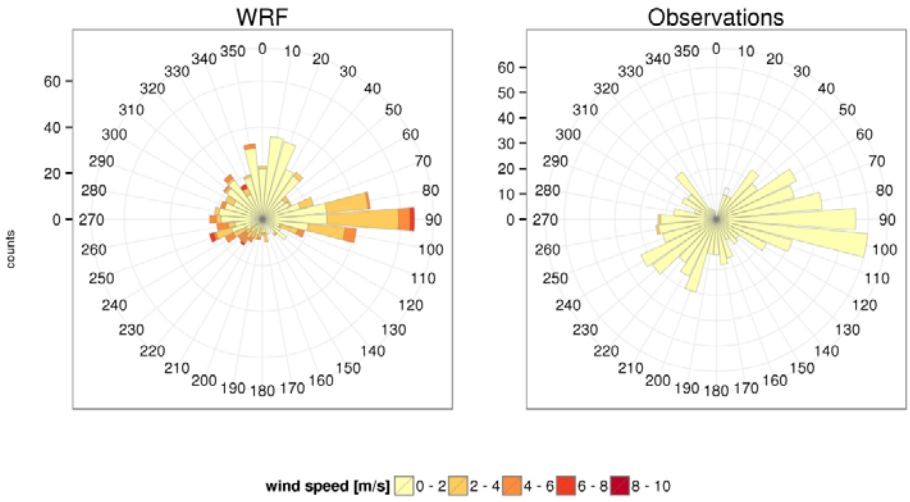

Figure 4: Wind directions in 10 degree sectors and wind speed classes simulated by WRF (left) and measured at the air quality monitoring station Klagenfurt Koschatstraße, situated in the city centre (right). The WRF distribution gives the grid point values, which are closest to the observation point.

The emission database

To model air quality successfully, the availability of detailed and up-to-date emission data is essential. Various datasets were thus combined, supplemented, modelled or processed to fulfil the modelling requirements (e.g., various spatial scales), to harmonise the data bases and to improve the emission data quality (for details see Uhrner et al., 2014).

For the European scale, the MACC (Monitoring Atmospheric Composition and Climate[3]) data set (Kuenen et al., 2011) was used, which features a resolution of about 7.5 km x 7.5 km. Emissions are assigned to so-called SNAP classes (Selected Nomenclature for Sources of Air Pollution; EEA, 2002). The relevant classes for this study are SNAP 07 for traffic emissions and SNAP 10 for agricultural emissions. MACC data were used as base data for the study and when no better resolved emission data were available.

[3] http://www.gmes-atmosphere.eu/data (2014-07-30)

The European data set was improved with regional emission data provided by the PMinter project partners. Improved regional emission data were mainly used for the SNAP classes of power generation, residential heating, commerce and industry, and agriculture. Emissions of these classes comprise chemical compounds such as SO_2, CO, NO_x, NMVOC, NH_3 and PM10.

Traffic emissions were handled separately. They were processed by IVT/TU Graz based on road network and traffic volume data provided by the project partners by means of the NEMO model (Rexeis and Hausberger, 2009; Rexeis and Hausberger, 2005).

All emission data were processed to fulfil the requirements as input data to WRF-Chem as specified in the WRF-Chem user guide (Peckham et al., 2013).

Emission scenarios to study the influence of emissions from traffic and agriculture

In the PMinter project, a multitude of scenarios was analysed to assess the impact of measures defined in air quality management plans. Here, the focus is on two emission scenarios, which affect traffic and agriculture.

The main emission source of nitrogen oxides within the target areas is road traffic. NO_x shows very high emission densities in cities and close to major routes (see Figure 5, left; the large rectangles in the lower right corner are due to the coarse MACC input data from Croatia). Acting as precursors for secondary aerosols, they are involved in the formation of nitric acid (HNO_3), which in turn may react rather quickly with NH_3 to form ammonium nitrate (NH_4NH_3). Ammonium nitrate plays an important role as secondary aerosol in the cold season, but dissociates again at higher temperature or low relative humidity related to low NH_3 and HNO_3 gas phase concentrations. As NO_2 has an atmospheric residence time of some days, it can be transported to more remote regions, where it can further react to form HNO_3. In the end, with NH_3 emissions from agriculture, which has an average atmospheric residence time of 10 about days (Wallace and Hobbs, 2006) NH_4NH_3 PM is formed. In Austria NH_3 emissions originate predominately from agriculture; the largest share is due to manure management of swine and cattle. The total share of agriculture in national NH_3 emissions amounted to 94 % in 2012 (Anderl et al., 2014). In the PMinter region, pig fattening and to a lesser extent dairy farming are important. Thus, the highest NH_3 emissions can be found in the rural areas of Styria and northern Slovenia, see Figure 5, right. It should be noted that—due to CPU costs—the non-linear aqueous phase cloud chemical processes, which lead to secondary particulate sulphate aerosols formation, was not included in the simulation. Thus SO_4^{2-} concentrations can be expected to be underestimated and NO_3^- concentration to be overestimated (Uhrner et al., 2014). However, the total amount of SO_2 emissions of the PMinter emission inventory can be regarded as small (Uhrner et al., 2014).

To study the influence of traffic NO_x emissions on PM and SIAs, an emission scenario with a reduction of 35 % NO_x emission originating from traffic was considered. This scenario is hereinafter referred to as ScNOx. The influence of agricultural NH_3 emissions is studied via a scenario, in which agricultural NH_3 emissions were reduced by 35 %. This scenario is hereinafter referred to as ScNH3. As reference to the reduction scenarios, a so-called base case, including 100 % of emissions in all SNAP classes, was simulated.

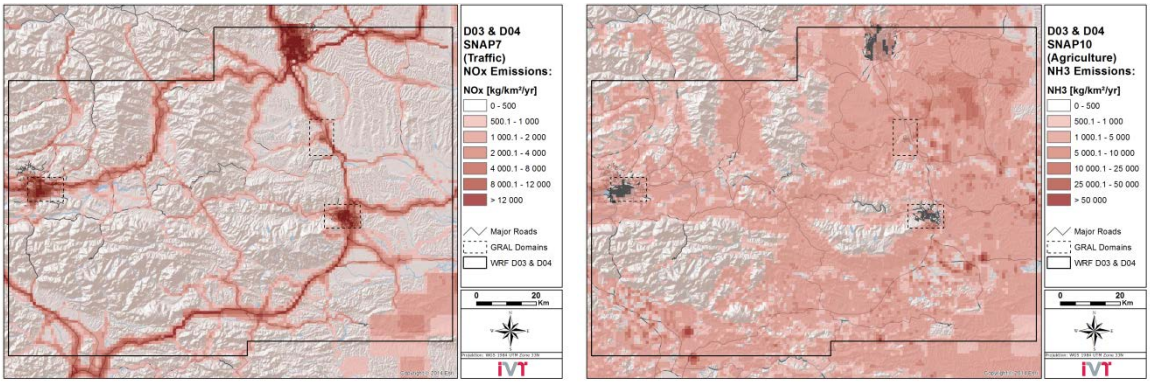

Figure 5: Traffic NO_x emissions (left) and agricultural NH_3 emissions (right) per year in the PMinter region. The spatial resolution of data is 1 km x 1 km.

3. Results of simulations and discussion with respect to PM and SIA

The structure of total primary PM10 emissions (not shown), as provided by the improved PMinter emission data base, shows a strong spatial variability and seems to be dominated by domestic-heating emissions. Figure 6, left, shows total PM10 concentration levels for January 2010 as simulated by WRF-Chem. Compared to the emission data, the spatial concentration distribution is much smoother, with highest values close to city centres and densely populated areas. The simulated PM10 concentrations are, as it can be expected due to high wind speeds simulated by WRF and due to resolution aspects, considerably lower than the measurements at air quality monitoring station. The 3 micro-scale areas are indicated and the results are discussed for Graz which lies at the edge of D03b domain. In Graz, e.g., monthly mean January 2010 measurements ranged between 46 µg m^{-3} at the station Graz-Nord and 62 µg m^{-3} the station Graz-Süd (Schopper et al., 2010), while WRF-Chem achieved for this area mostly 30 µg m^{-3} to 40 µg m^{-3} (the simulated maximum grid-point value amounts to 42 µg m^{-3}). Nevertheless, the model succeeds to capture the still coarse (1 x 1 km) spatial PM10 distribution sufficiently well. Compared to the coarser resolved domain D02 (not shown), the 1 km x 1 km resolved simulations show more detail and more realistic values with respect to local maxima and minima of concentration levels. Figure 6, right, depicts the simulated share of SIAs in total PM10 concentrations. A first glance at the figure reveals that the share of SIAs is lower in and close to cities or remote and higher elevated regions, but amounts to at least 50 % in rural areas. In general, higher values are obtained in the eastern part of the PMinter region.

The simulated NO_2 and NH_3 concentration levels for the base case exhibit a pattern, which is similar to the emissions of NO_x and NH_3, shown in Figure 5. In contrast to the emissions, the concentrations become spatially more blurred. Base case NH_3 concentration levels are generally remarkably lower in the western part of the PMinter project region, i.e., in Carinthia. There, NH_3 concentrations average to about 0.5 µg m^{-3}. Over almost all area of Styria and eastern Slovenia, NH_3 concentrations range between about 1 µg m^{-3} and 10 µg m^{-3}. This reflects the emission situation. In Carinthia, NH_3 emissions are constrained to the basin of Klagenfurt and the valleys and do not exceed 5000 kg/(km² year), while in Styria and large parts of Slovenia emissions are found region-wide and reach values of up to 25,000 kg/(km² year).

NO_2 concentrations levels are also generally lower in the western PMinter region, except for the micro-scale region of Klagenfurt. In Styria and eastern Slovenia, base case NO_2 concentration levels exceed almost everywhere 20 µg m^{-3}. In Carinthia and western Slovenia, these values are only achieved in valleys along major routes.

The SIA NH_4NO_3 formation process from NO_x and NH_3 emissions can be roughly described by two reactions: (1) $NO_2 + OH \rightarrow HNO_3$, and (2) $HNO_3 + NH_3 \rightarrow NH_4NO_3$. The formation of the direct precursors gas HNO_3 (1) is related to photochemical processes and HNO_3 formation shows maximum values with maximum solar radiation (normally around noon). In general, high SIA concentrations require high NO_2 and low HNO_3 concentrations as a prerequisite, i.e., there is enough NO_2 and NH_3 available to form SIAs. In Styria and Slovenia, high SIA concentrations go hand in hand with high NH_3 levels.

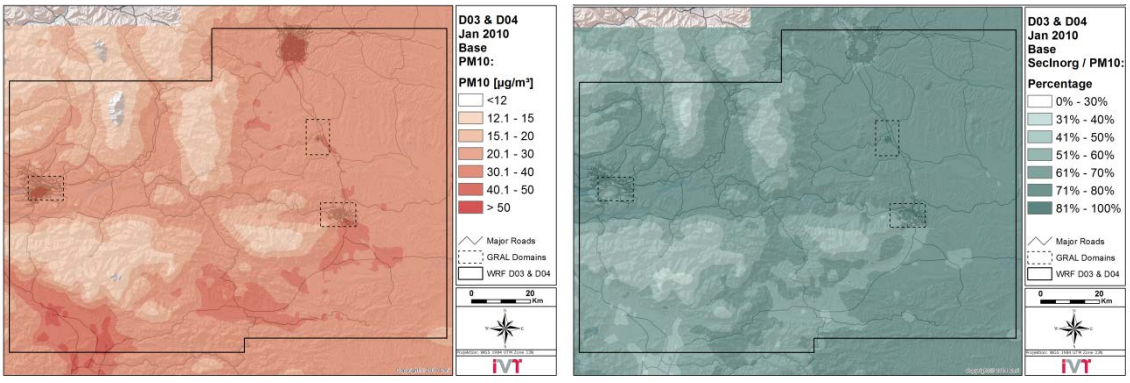

Figure 6: PM10 concentration levels (left) and the share of secondary inorganic aerosols in PM10 (right) for the base case

The formation and evaporation of SIA behaves strongly non-linear, depending on various processes, such as concentration levels of precursors, particle concentration, deposition velocities (higher for HNO_3 and NH_3 than for PM10) and ambient conditions (temperatures and humidity).

Results of the NO_x reduction scenario (ScNOx)

Reducing NO_x emissions by 35 % leads, as expected, to decreased NO_2 concentrations (approx. –1 µg m^{-3} to –5 µg m^{-3}) around regions which are strongly influenced by traffic (see Figure 7, which depicts differences between the simulated concentration levels from ScNOx and base case for NO_2 as well as for NH_3, HNO_3 and SIA). However, concentrations of the final precursor gas HNO_3, nitrate and ammonium and hence PM10 are only negligibly influenced.

As a consequence of reduced NO_2, HNO_3 concentrations drop in those areas, which showed higher HNO_3 concentration levels in the base case and which are located rather in valleys and basins; in contrast, high base case HNO_3 concentrations, which were found over mountainous areas, are rarely reduced. These retaining higher concentrations over mountains may be induced by lower deposition velocities over snow (Gauglustaine et al., 1994) or by competing reactions consuming the OH radical necessary for the NO_2 to NHO_3 reaction. In general, the HNO_3 reduction is very small and amounts to about – 0.15 µg m^{-3} or less. In the eastern PMinter region, base case HNO_3 concentrations are nearly zero, thus there is no potential for changes due to NO_x emission reduction in this area.

The regions, which show low HNO_3 base concentrations, coincide with regions of high NH_3 concentrations (which are also found in some agricultural regions in Carinthia, such as the Lavanttal and the basin around Klagenfurt and in Slovenia the region north of Ljubljana). Thus, it can be assumed that there most HNO_3 reacts with NH_3 to form SIA. The ScNOx does not alter the emission levels of NH_3. As less NO_2 and thus HNO_3 is available, less NH_3 can be transformed into SIA. Therefore, the NH_3 concentration levels increase very slightly with respect to the base case in regions with high NH_3 emissions by up to 0.02 µg m^{-3}.

The impact on SIA concentrations (which is identical to the PM10 changes) due to the 35 % emission reduction of NO_x is marginal and limited to regions, where NH_3 are high and NH3 is in abundance (rural areas in Styria and eastern Slovenia) see Figure 7, bottom right.

To obtain an estimate for the concentration level changes in the scenarios as simulated by WRF-Chem, the average concentration change at all grid-points belonging to each of the micro-scale focus regions was calculated.

The ScNOx yielded average NO_2 reductions of about –2 µg m^{-3} in Leibnitz, about –3 µg m^{-3} in Maribor and about –3.6 µg m^{-3} in Klagenfurt. The resulting average SIA reduction is equivalent to the PM10 reduction and amounts to negligible changes (–0.01 µg m^{-3}) in the micro-scale areas (–0.02 µg m^{-3} in Klagenfurt). These values are on a par with the average NH_3 increase in the micro-scale areas.

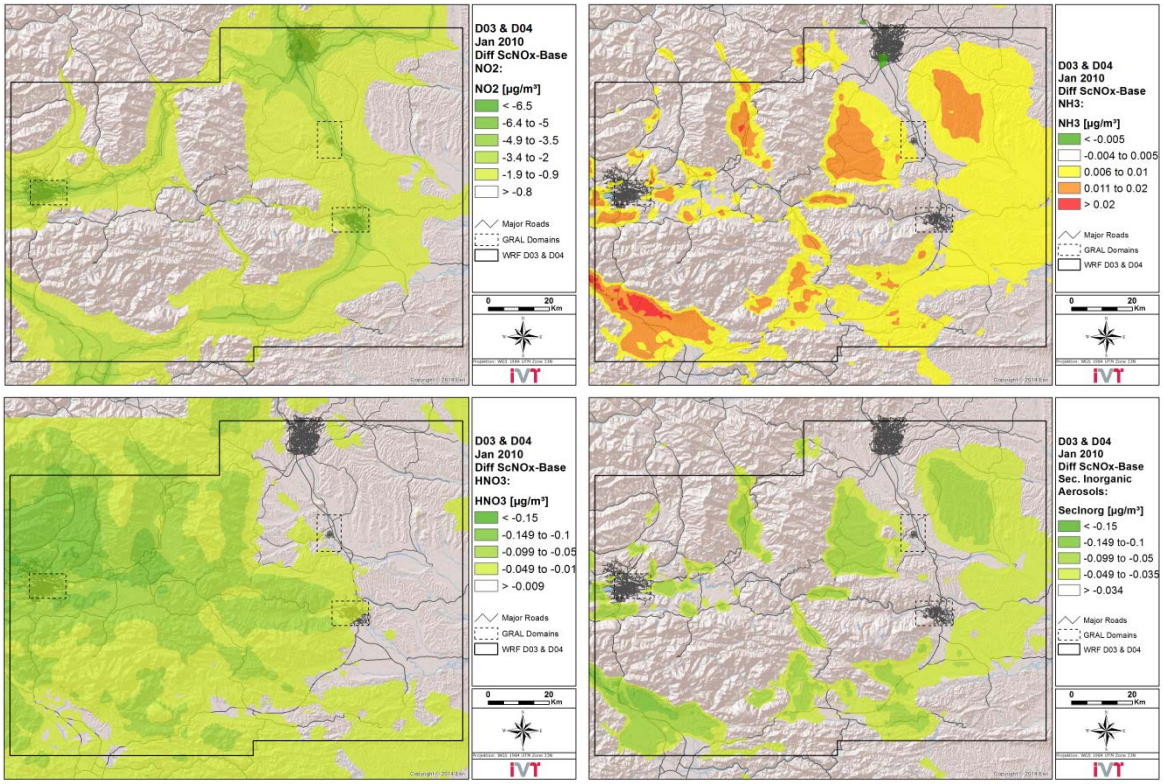

Figure 7: Concentration differences between ScNOx minus Base for NO_2 (top left), NH_3 (top right), HNO_3 (bottom left) and SIA (bottom right)

In summary, the 35 % NO_x emission reductions lead to negligible SIA concentration decreases. Those are highest in rural regions with already high or additional NH_3 concentration levels and amount there at most to –0.15 µg m^{-3}

Results of the NH_3 reduction scenario (ScNH3)

For the NH_3 reduction scenario, all agricultural NH_3 emissions were reduced by 35 %. NH_3 emissions are particularly high in the eastern part of the PMinter region. In Carinthia, notable emissions are lower and restricted to the Lavanttal and the basin of Klagenfurt. Thus, the NH_3 emission reduction leads—with respect to the base case—to a considerable and extensive decrease of NH_3 concentration in the Styrian and eastern Slovenian PMinter areas, amounting between at least –0.5 µg m^{-3} and up to –4 µg m^{-3} (see Figure 8, which depicts changes in NO_3^-, NH_3, HNO_3 and SIA due to reduction of NH_3 emissions). Similar high reduction values are found north of Ljubljana and around Celje. The highest average change in the micro-scale areas is found for Leibnitz with about –1 µg m^{-3}, mean reduction in Maribor amounts to –0.32 µg m^{-3} and in Klagenfurt to –0.12 µg m^{-3}.

In addition to NH_3, $NH4^+$ and NO_3^- PM decreases as well, while HNO_3 increases due to the complex gas/particle equilibrium thermodynamics. NH_4^+ and NO_3^- changes are strongest in the basins and valleys in Carinthia and lessen when steering eastwards. The changes amount up to –3.5 µg m^{-3} in same parts of the basin of Klagenfurt and to around –1.5 µg m^{-3} in eastern Styria. In contrast to the other SIA precursors, HNO_3 reacts to NH_3 emission reduction with higher concentration levels, particularly in the same regions, where NO_3^- declines. This abundance of HNO_3 accounts for the decrease of SIA in the same regions.

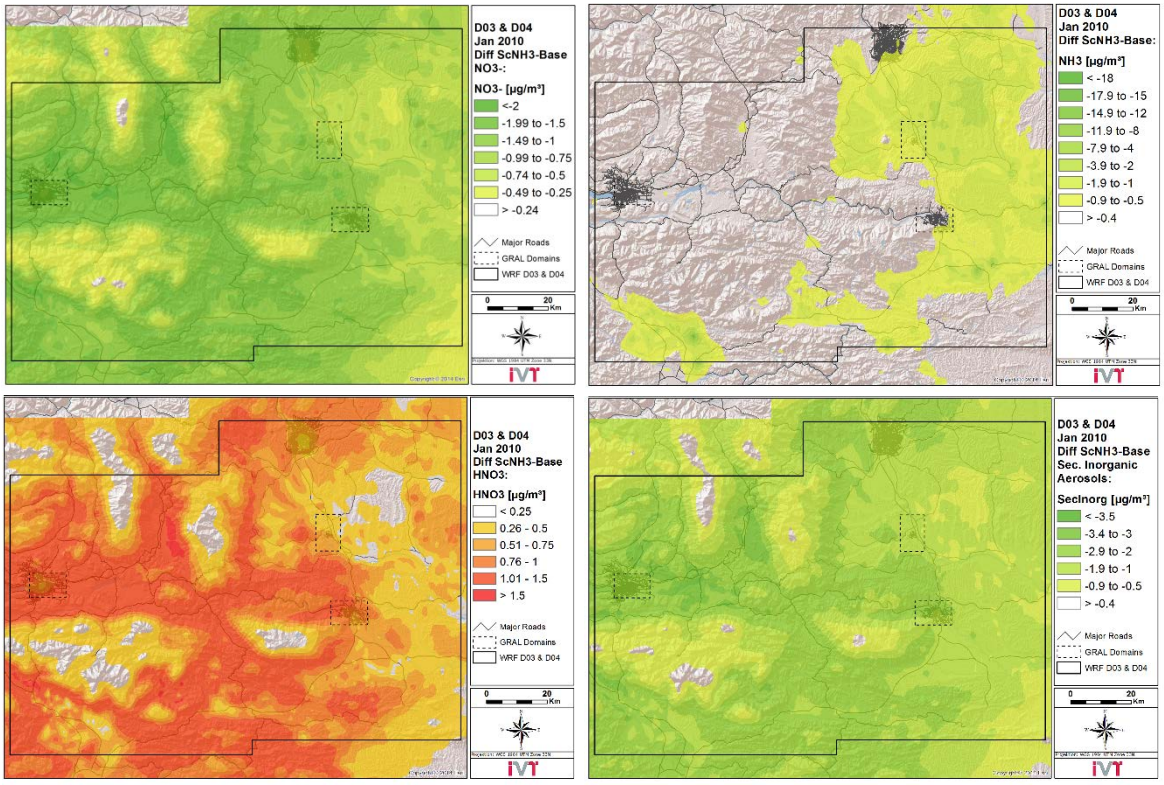

Figure 8: Concentration differences between ScNH3 minus Base for NO_3^- (top left), NH_3 (top right), HNO_3 (bottom left) and SIA (bottom right). Mind the different color scales with respect to Figure 7.

In contrast to the ScNOx, reducing NH_3 leads to considerable changes in SIA and PM10 concentrations. The average SIA reductions in the three micro-scale areas are strongest in Klagenfurt, where it amount to –2.7 µg m^{-3}, followed by Maribor with –2.1 µg m^{-3} and Leibnitz with –1.6 µg m^{-3}. Thus, the reduction potential is higher in regions with rather low changes in NH_3 concentrations and vice versa. The SIA decrease is similar to the PM10 reduction potential.

Discussion of the Results

The simulated PM concentration results, as presented above, show different sensitivity and response of SIA formation with respect to NO_x and NH_3 emission changes.

To understand the sensitivity of a region to NO_x and NH_3 related measures, the base case molar ratio of HNO_3 to NH_3 can be used as a key parameter[4]. This ratio can be considered as to represent in first approximation the free acid and alkaline components, as cloud aqueous phase chemical processes were not incorporated in the WRF-Chem simulations. Similar to a study by Uhrner et al. (2006), base case HNO_3 to NH_3 ratios << 1 should identify areas sensitive to NO_x related measures, i.e., alkaline components are in excess; HNO_3 to NH_3 ratios >> 1 should identify areas sensitive to NH_3 related measures, i.e., acid components are in excess.

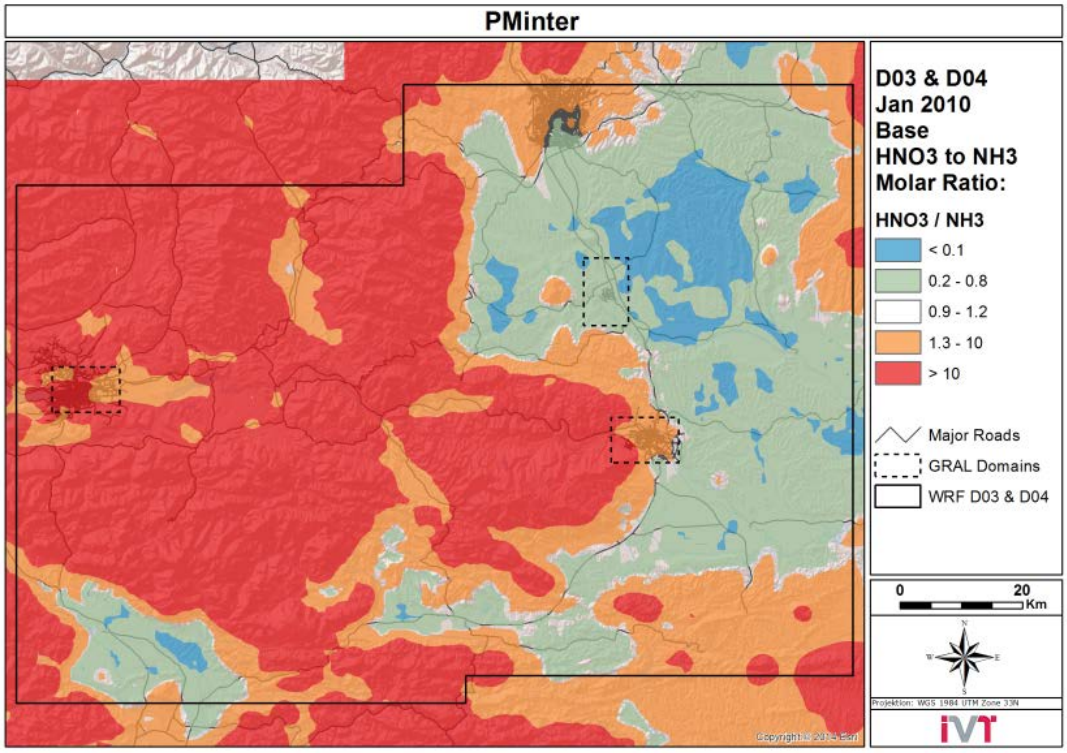

Figure 9: HNO_3 to NH_3 molar ratio for the base case. Areas generally sensitive to NO_x measures (i.e., ratios are well below one) are predominantly found in the eastern PMinter region and in Slovenian areas, which show high NH_3 emissions due to agriculture (south and east from Maribor, around Celje and north of Ljubljana). Regions which are generally more sensitive to NH_3 measurements are found in Carinthia, in and around Klagenfurt (there, NH_3 emissions are generally lower than in Styria and Slovenia).

Figure 9 shows the molar HNO_3 to NH_3 ratio for the base case. Areas generally sensitive to NO_x measures (i.e., ratios are well below one) are predominantly found in the eastern PMinter region and in Slovenian areas, which show high NH_3 emissions due to agriculture (south and east from Maribor, around Celje and north of Ljubljana). Regions which are generally more sensitive to NH_3 measurements are found in Carinthia, in and around Klagenfurt (there, NH_3 emissions are generally lower than in Styria and Slovenia).

NO_x and following NO_2 reductions did finally only lead to minor HNO_3 reductions and also minor nitrate changes (not shown), resulting in only very small PM10 (and SIA) reductions. These small changes can mainly be found in the rural areas of Styria and Slovenia and to an even much lesser account around Klagenfurt and in the Lavanttal (see Figure 7, bottom right) and coincide with those regions, which show a general NO_x sensitivity via the HNO_3 to NH_3 ratio (ratio values of about 0.1), as shown in Figure 9.

[4] This mass ratio is given as HNO_3 divided by NH_3 (both in ppbv):

In contrast to the NO_x reduction scenario, the NH_3 reduction scenario shows an area-wide and much more pronounced SIA and PM10 decrease. Highest SIA decreases are found in areas with low to medium NH_3 emissions, with the exception of mountainous areas, where no significant impact appears. The ScNH3 is most effective, where the HNO_3 to NH_3 ratio ranges from 1 to 10 (in mountainous areas, the ratio is mostly above 10). Small effects occur in areas with high NH_3 concentrations and HNO_3 to NH_3 ratios below 0.1.

4. Summary

In this study, the regional impact of emission reductions of NO_x from traffic and NH_3 from agriculture for SIA and PM10 was studied for an exemplary winter month, i.e., January 2010. Focus regions was southern Austria and large parts of Slovenia, a region, where PM10 EU and national limit exceedances occur frequently in the cold season.

A detailed emissions data base was established for the study area and WRF-Chem, a sophisticated chemical transport model, was used to model the dispersion and chemistry of air pollutants. WRF-Chem proved to be capable of representing rural, near-city and in urban background at a horizontal resolution of 1 km x 1 km reasonably well.

This study focused on January 2010. Due to different emission activities and ambient conditions, these results cannot be projected to other seasons. In addition to the seasonal cycle of NH_3 emissions, different prevailing flow conditions and different temperature and humidity regimes, reduction potentials may differ from the January 2010 values. Nevertheless, several studies indicated a high reduction potential for SIA due to reduced NH_3 emissions, e.g., Banzhaf et al. (2013), Derwent et al. (2009).

To study the potential to decrease the PM burden in the region, WRF-Chem results of two scenarios were compared to those from a base case, including all expectable emissions. With respect to SIA and PM10 reduction, the –35 % NH_3 scenario turned out to be the most efficient measure. However, it must be noted that due to the particle ion balance and the semi-volatile behaviour of NH_4NO_3, NH_3 emission reductions lead in the end to combined reductions of particulate NH_4^+ and NO_3^-, and the latter component originates from traffic sources. Due to the molar weights ratio of HNO_3/NH_3 of 3.7, comparatively small mass based NH_4^+ changes may result in high NO_3^- mass changes

The base case molar ratio of HNO_3 to NH_3 proved useful to ease the interpretation of the simulation results, as it represents in first approximation information about free acid and alkaline precursors. Thus, it can be used to identify regions sensitive to NO_x related measures (ratio around 0.1) and to NH_3 related measures (ratio between 1 and 10). The emission regimes and in consequence the component concentrations in the study area vary. Although large and predominantly rural areas in Styria and Slovenia are characterized by an ammonia and ammonium abundance, which comes along with a low total nitrate to total ammonia ratio, only negligible PM10 reductions of at most –0.15 µg m^{-3} were computed along with the NO_x reduction scenario. This is due to only minor HNO_3 reductions, even though NO_x decreased significantly and over large areas. HNO_3 formation and conservation is not only diminished by transport and dilution of precursors, but also by a relatively high level of deposition. All these highly non-linear processes are captured by WRF-Chem. The response of SIA to NH_3 reductions was related to areas with a molar HNO_3 to NH_3 ratio of 1 to 10 and resulted in much more pronounced PM10 decreases of (–2 to –4) µg m^{-3} in these areas.

In conclusion, any measure to be taken to reduce NH_3 from agriculture is likely to be much more effective to ease the PM burden in the study region than any reduction in NO_x from road traffic. Nevertheless, reducing NO_x emissions from traffic leads to area-wide NO_2 reductions of (–2 to –4) µg m^{-3} and thus implies a substantial positive effect on health issues in the region.

Acknowledgements

This work was supported by the EU interregional SI-AT-2-2-047 programme and co-financed by the provincial government of Styria.
We thank the project partners for fruitful discussions and making available various data which helped to establish a multi-scale emission database for the project region and for various air quality and observational data. All these data formed the basis for the successful air quality modelling work and helped us to validate the simulation results.
The authors wish to thank Martin Rexeis and Martin Dippold from IVT for the NEMO support, Hugo Denier van der Gon for the provision of MACC data. We thank ECMWF for making available ERA-Interim data and Manfred Stepponat (TUG) and the VSC team in Vienna for the great support and the computing time on the Vienna Scientific Cluster.

References

Anderl A., S. Haider, H. Jobstmann, E. Kampel, T. Köther, C. Lampert, L. Moosmann, K. Pazdernik, M. Pinterits, S. Poupa, G. Stranner and A. Zechmeister (2014), Austria's Informative Inventory Report (IIR) 2014. Submission under the UNECE Convention on Long-range Transboundary Air Pollution*, REP-0474, Umweltbundesamt Wien*, 1–367.

Banzhaf S., M. Schaap, R.J. Wichink Kruit, H.A.C. Denier van der Gon, R. Stern and P.J.H. Builtjes (2013), Impact of emission changes on secondary inorganic aerosol episodes across Germany*, Atmospheric Chemistry and Physics, 13*, 11675–11693.

Chen F. and J. Dudhia (2001), Coupling an advanced land surface-hydrology model with the Penn State-NCAR MM5 modeling system. Part I: Model implementation and sensitivity*, Mon.Weather Rev., 129*, 569–585.

Chou M. and M.J. Suarez (1994), An efficient thermal infrared radiation parameterization for use in general circulation models*, NASA Tech. Memo., 104606*, 85.

Dee D.P., S.M. Uppala, A.J. Simmons, P. Berrisford, P. Poli, S. Kobayashi, U. Andrae, M.A. Balmaseda, G. Balsamo and P. Bauer (2011), The ERA-Interim reanalysis: Configuration and performance of the data assimilation system*, Q.J.R. Meteorol. Soc., 137*, 553–597.

Derwent R., C. Witham, A. Redington, M. Jenkin, J. Stedman, R. Yardley and G. Hayman (2009), Particulate matter at a rural location in southern England during 2006: model sensitivities to precursor emissions*, Atmos. Environ., 43*, 689–696.

ECE (2008), Directive by the European Parliament and Council of the European Union on ambient air quality and cleaner air for Europe*, 2008/50/EC*.

EEA (2002)*, EMEP/CORINAIR Emission Inventory Guidebook – 3rd edition*, European Environment Agency.

Grell G.A., S.E. Peckham, R. Schmitz, S.A. McKeen, G. Frost, W.C. Skamarock and B. Eder (2005), Fully coupled “online” chemistry within the WRF model*, Atmos. Environ., 39*, 6957–6975.

Grell G.A. and D. Dévényi (2002), A generalized approach to parameterizing convection combining ensemble and data assimilation techniques*, Geophys. Res. Lett., 29*, 38-1-38-4.

Hauglustaine, D. A., Granier, C., Brasseur, G.P., and Megie, G. (1994), The importance of atmospheric chemistry in the calculation of radiative forcing on the climate system, J. Geophys. Res. 99, 1173-1186.

Hong S., Y. Noh and J. Dudhia (2006), A new vertical diffusion package with an explicit treatment of entrainment processes*, Mon. Weather Rev., 134*, 2318–2341.

IG-L (2011), Gesamte Rechtsvorschrift für Immissionsschutzgesetz - Luft*, BGBl. I Nr. 115*.

Kuenen J., H.D. van der Gon, A. Visschedijk, H. van der Brugh and R. van Gijlswijk (2011), MACC European emission inventory for the years 2003–2007*, TNO-report*.

Lin Y., R.D. Farley and H.D. Orville (1983), Bulk parameterization of the snow field in a cloud model*, Journal of Climate and Applied Meteorology, 22*, 1065–1092.

Mlawer E.J., S.J. Taubman, P.D. Brown, M.J. Iacono and S.A. Clough (1997), Radiative transfer for inhomogeneous atmospheres: RRTM, a validated correlated-k model for the longwave*, Journal of Geophysical Research: Atmospheres, 102*, 16663–16682.

Oettl D. and U. Uhrner (2012), Documentation of the Lagrangian Particle Model GRAL (Graz Lagrangian Model) Vs. 12.5*, Amt d. Stmk. Landesregierung, FA17C, Technische Umweltkontrolle, Bericht Lu-03-12*.

Oettl D., P.J. Sturm, G. Pretterhofer, M. Bacher, J. Rodler and R.A. Almbauer (2003), Lagrangian dispersion modeling of vehicular emissions from a highway in complex terrain*, J. Air Waste Manage. Assoc., 53*, 1233–1240.

Peckham S.E., G. Grell, S.A. McKeen, R. Ahmadov, J. Fast, W.I. Gustafson, S.J. Ghan, R. Zaveri, R.C. Easter, J. Barnard, E. Chapman, R. Schmitz, M. Salzmann, V. Beck, M. Barth, G. Pfister, C. Wiedinmyer, M. Heweson and S.R. Freitas (2013)*, WRF-Chem Version 3.5 User’s Guide*, National Center for Atmospheric Research (NCAR).

Rexeis M., and S. Hausberger (2005), Calculation of Vehicle Emissions in Road Networks with the model “NEMO”*, 14th Symposium Transport and Air Pollution, 85/I*, 118–127.

Rexeis M. and S. Hausberger (2009), Trend of vehicle emission levels until 2020–Prognosis based on current vehicle measurements and future emission legislation*, Atmos. Environ., 43*, 468–94698.

Schell B., I.J. Ackermann, H. Hass, F.S. Binkowski and A. Ebel (2001), Modeling the formation of secondary organic aerosol within a comprehensive air quality model system*, Journal of Geophysical Research: Atmospheres, 106*, 28275–28293.

Schopper A., G. Zelisko and M. Gassenburger (2010), Ergebnisse aus dem steirischen Immissionsmessnetz*, Monatlicher Luftgütebericht Jänner 2010*, 46.

Spangl W., and C. Nagl (2012), Jahresbericht der Luftgütemessungen in Österreich 2011*, REP-0383, Umweltbundesamt Wien*, 1–180.

Spangl W., and C. Nagl (2011), Jahresbericht der Luftgütemessungen in Österreich 2010*, REP-0326, Umweltbundesamt Wien*, 1–175.

Spangl W., and C. Nagl (2010), Jahresbericht der Luftgütemessungen in Österreich 2009*, REP-0261, Umweltbundesamt Wien*, 1–176.

Spangl W., and C. Nagl (2009), Jahresbericht der Luftgütemessungen in Österreich 2008*, REP-0231, Umweltbundesamt Wien*, 1–191.

Spangl W., C. Nagl, J. Schneider and A. Kaiser (2006), Herkunftsanalyse der PM10-Belastungen in Österreich. Ferntransport und regionale Beiträge*, REP-0034, Umweltbundesamt Wien*, 1–112.

Stockwell W.R., P. Middleton, J.S. Chang and X. Tang (1990), The second generation regional acid deposition model chemical mechanism for regional air quality modeling*, Journal of Geophysical Research: Atmospheres, 95*, 16343–16367.

Uhrner U., B.C. Lackner, R. Reifeltshammer, M. Steiner, R. Forkel and P.J. Sturm (2014)*, Inter-Regional Air Quality Assessment - Bridging the Gap between Regional and Kerbside PM Pollution. Results of the PMInter Project (Final Report)*, Graz, Institute for Internal Combustion Engines and Thermodynamics.

Uhrner U., S. Drechsler, R. Wolke, R. Lumpp, D. Ahrens and A. Wiedensohler (2006), Sensitivity of urban and rural Ammonium-Nitrate PM to Precursor Emissions in Southern Germany*, 10th ETH-Conference on Combustion Generated Nanoparticles, Zürich*.

Wallace J.M. and P.V. Hobbs (2006)*, Atmospheric science: an introductory survey*, Academic press.